Optical Study of Flow and Combustion in an HCCI Engine with Negative Valve Overlap

Trevor S. Wilson, Hongming Xu, Steve Richardson

Jaguar Cars Ltd., Whitley Engineering Centre, Coventry. CV3 4LF

twilso80@jaguar.com

Miroslaw L. Wyszynski, Thanos Megaritis

The University of Birmingham, Edgbaston, Birmingham. B15 2TT

One of the most widely used methods to enable Homogeneous Charge Compression Ignition (HCCI) combustion is using negative valve overlapping to trap a sufficient quantity of hot residual gas. The characteristics of air motion with specially designed valve events having reduced valve lift and durations associated with HCCI engines and their effect on subsequent combustion are not yet fully understood. In addition, the ignition process and combustion development in such engines are very different from those in conventional spark-ignition or diesel compression ignition engines. Very little data has been reported concerning optical diagnostics of the flow and combustion in the engine using negative valve overlapping. This paper presents an experimental investigation into the in-cylinder flow characteristics and combustion development in an optical engine operating in HCCI combustion mode. PIV measurements have been taken under motored engine conditions to provide a quantitative flow characterisation of negative valve overlap in-cylinder flows. The ignition and combustion process was imaged using a high resolution charge coupled device (CCD) camera and the combustion imaging data was supplemented by simultaneously recorded in-cylinder pressure data which assisted the analysis of the images. It is found that the flow characteristics with negative valve overlapping are less stable and more valve event driven than typical spark ignition in-cylinder flows, while the combustion initiation locations are not uniformly distributed.

1. Introduction

Homogeneous Charge Compression Ignition engines hold the potential to significantly reduce Oxides of Nitrogen (NOx) emissions and improve fuel consumption of automotive engines. Negative valve overlapping has been widely used to enable the so-called 'controlled auto-ignition' and this arrangement has been researched along with hydrogen addition by the authors previously [1]. There are many experimental techniques that have been applied and are available to detect and either quantify or qualify flow conditions prevailing before the onset of combustion. These include flow visualisation, PIV [3,5], particle tracking velocimetry (PTV) [6] and Laser Doppler Anemometry (LDA) [4]. There also exist many techniques that can detect combustion phenomena such as ionisation probe sensors and Laser Induced Florescence (LIF) [7,9]. The characteristics of air motion with specially designed valve events having reduced valve lift and durations associated with HCCI engines have also been studied using CFD simulations, but limited experimental data is available of the in-

cylinder flow process. Direct optical observation of the combustion is one of the most capable methods to visualise and understand the in-cylinder combustion process. The typical combustion characteristics observed using combustion visualisation include combustion initiation location, flame front shape and flame speed. HCCI combustion imaging has previously been performed by Hultquist *et.al.* in 2002 [2] who performed simultaneous fuel tracer LIF and chemiluminescence imaging to study the HCCI development process within one cycle as compared to SI combustion. Relatively less information is available concerning the optical measurement of combustion in HCCI engines operating with negative valve overlap.

This paper presents an experimental investigation of the characteristics of in-cylinder flow and combustion development in an optical HCCI engine with negative valve overlapping. PIV measurements have been taken under motored engine conditions and a quantitative analysis has been carried out to characterise the flow with negative valve overlap conditions. A high resolution charge coupled device (CCD) camera was used to take images of the combustion. The imaging data was supplemented by simultaneously recorded in-cylinder pressure data which assisted the analysis of the combustion development. The experimental systems are described in the next section and the measurement results are then presented and discussed, with a summary of findings at the end of the paper.

2. Experimental System

A single cylinder version of the Jaguar 2.5L V6 engine, **Figure 1**, was built with optical access possible through the extended (bowditch design) piston with 65mm quartz window viewed off a 45° stationary mirror, barrel (bore: 81.64mm, either long or short liner) and through a quartz window that could be inserted in the vertical wall of the pentroof. The engine had compression ratio (CR) of 12.9:1 and was fitted with 150° duration, low lift camshafts for HCCI operation; HCCI was enabled utilising the symmetrical negative valve overlapping technique. The engine geometry details are shown in Table 1.
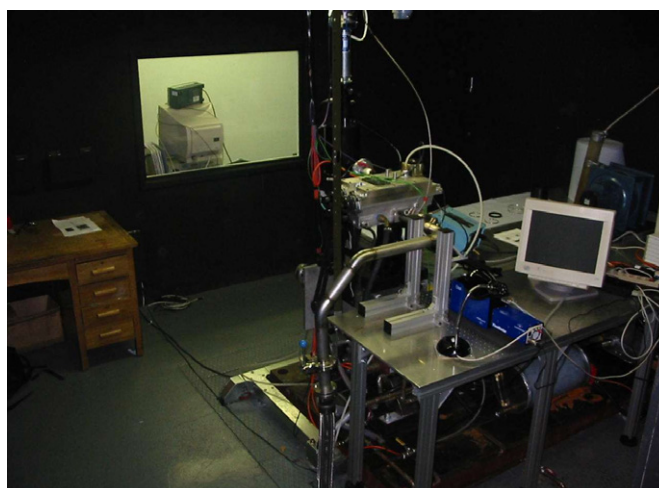

Figure 1. Optical engine cell.

The charge was fed to a standard inlet port through an air filter, rotary gas volumetric flow meter, manual throttle, intake heater and plenum. The intake heater, required for enabling HCCI combustion of natural gas with the low CR of 12.9:1, consisted of a 3kW inline and 2kW band heaters capable of supplying a sustained heated intake temperature in excess of 250ºC at 1000 RPM with the low lift HCCI camshafts. An electronically controlled bypass system fed compressed air through the heaters to permit warm-up and cool down of the intake system without motoring the engine. This was isolated before cranking. Inlet air temperature was measured with a K-type thermocouple located just upstream of the inlet port. A PID controller compared this actual inlet temperature with the requested

temperature and cycled the heaters on and off appropriately. Air / Fuel Ratio (AFR) monitoring was provided with an ETAS™ lambda checker fitted approximately 1m downstream of the exhaust valves. The device indicated lambda to two decimal places.

Type:	4 valve / cylinder	Fuel added in intake port:	Natural gas
CR:	12.9:1	Intake temperature:	300 – 550 K
Bore:	81.64 mm	Typical Inlet MOP:	450-550°CA aTDC
Stroke:	79.5 mm	Typical Exhaust MOP:	180-250°CA aTDC

Table 1, Engine details.

For the PIV measurement, the flow was seeded with light-reflecting oil droplets. It is believed that the seeding accurately follows the internal flow structures. A thin laser light sheet was produced that defined a two-dimensional plane in the flow field, Figure 2. The LaVision FlowMaster PIV system was used which includes a dual frame CCD camera for cross-correlation PIV.
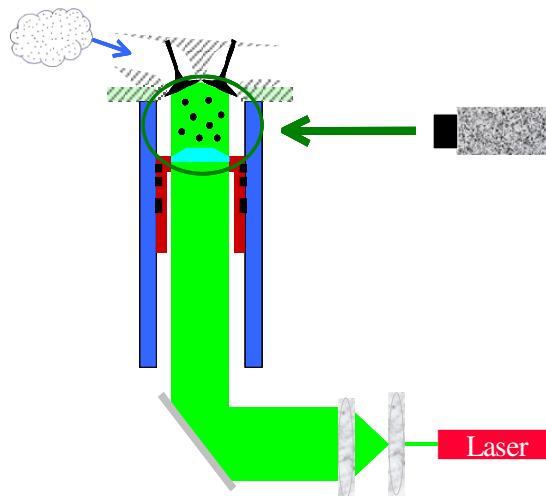

Figure 2. Schematic view of the PIV system setup.

In each case the light sheet was inserted through the centreline of the piston and was of thickness 1.1 mm ± 0.1 mm. The pulse duration was 10 ns and the pulses were separated by between 20 – 40 μs depending on flow velocity. The third velocity component could therefore reach 10 m/s with $^2/_3$ of the particles remaining within the sheet. As the third component is not expected to exceed this limit, it is anticipated that the calculated vectors are a realistic representation of the in-cylinder flow.

The raw particle image was corrected for the distortion introduced by the cylinder liner through software. The PIV processing utilised a multi-pass technique with an initial correlation at 128x128 pixels and a final pass with an interrogation region size of 32x32 pixels with a 50% overlap. Limited vector post processing was performed and was restricted to the removal of vectors with excessively large magnitudes.

The instrumentation used for the combustion imaging was an Andor iSTAR™, 1024x1024 pixel, intensified CDD camera with Nikkor UV lens. The spectral acceptance of the intensified camera system ranges from 180 to 850nm. The camera viewed the combustion chamber off a stationary 45° mirror mounted in the piston extension. The combustion piston was fitted with a 65 mm diameter silica window which is approximately 65% of the cylinder cross section, **Figure 3**. Such an experimental arrangement permitted a spatial resolution in the order of ½ mm, therefore these results will be referred to as 'high-resolution combustion imaging'.
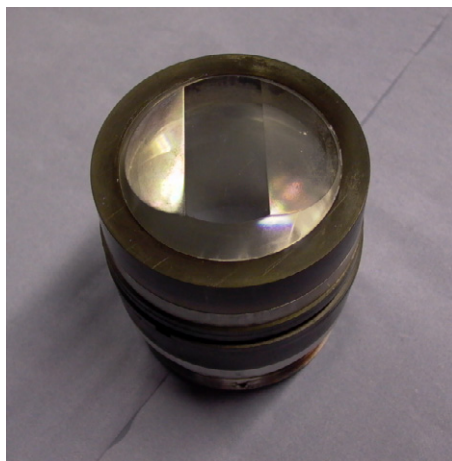

Figure 3. Photograph of the high-compression optical piston.

The engine was motored at the fixed speed of 1000 RPM. Valve events and fuelling that would provide a load of between 2.5 – 3.5 bar IMEP (Indicated Mean Effective Pressure, integrated over 720° CA) were chosen. The engine was started in SI and eased into HCCI mode through spark control for any auto-ignition tests. Intake temperature was controlled to maintain a consistent combustion phasing.

3. Results and Discussion

3.1. PIV measurements

The testing was performed at various engine conditions. For all valve and imaging timings, 0° is TDC gas exchange. Primarily, the aim of the PIV investigation was to establish the effect of the valve strategies involving large negative valve overlap (NVO) and short duration (and therefore also lower lift) on in-cylinder flow.

Results from a typical HCCI engine condition motored at 1000 RPM (case 1) are presented in **Figure 4**. The valve timing for this condition was 125/110 (IVO [deg CA aTDC]/EVC [deg CA bTDC]). The maximum magnitudes of the in-cylinder flow with NVO valve events were observed to be as high as around 20m/s (5 times mean piston speed) early in the intake stroke due to the reduced valve duration and lift. The flow velocity at the end of compression dropped to under 4 m/s (just under mean piston speed) during compression.

The results from case 2, the higher load condition (around 3.5 bar IMEP) HCCI case as determined by the symmetric valve timing of 105/105, are presented in **Figure 5**. In general the flow structures observed at this modified valve timing NVO case are similar to those observed at the valve timing of case 1 but it is not possible to compare the flow structures at 135 deg due to water vapour condensation in-cylinder during the intake stroke. However at 180 deg (**Figure 5**a) the flows showed some differences. First, due to the advanced intake valve timing over case 1, we no longer observe the higher velocity flow around the intake valve. Secondly, also due to the advanced valve timing, the

bulk flow structures off the piston have a higher flow magnitude. This is due to higher flow magnitudes earlier in the intake stroke.

In general the overall flow structure captured at 225 deg high load (not presented) appear very similar to that of the 225 deg standard case (not presented). Surprisingly, although the flow structure appears similar, and the magnitude of the tumble ratio is very similar, the tumble ratio now indicates rotation in the opposite direction (now anti-clockwise in the plane of the arrangement shown). The cause of this discrepancy is the direction of the bulk resultant flow at 225 deg that is dominant in the tumble ratio calculation.

Flow 45 degrees later at 270 deg (**Figure 5**b) is very similar to the flows observed in the standard case (**Figure 4**b).
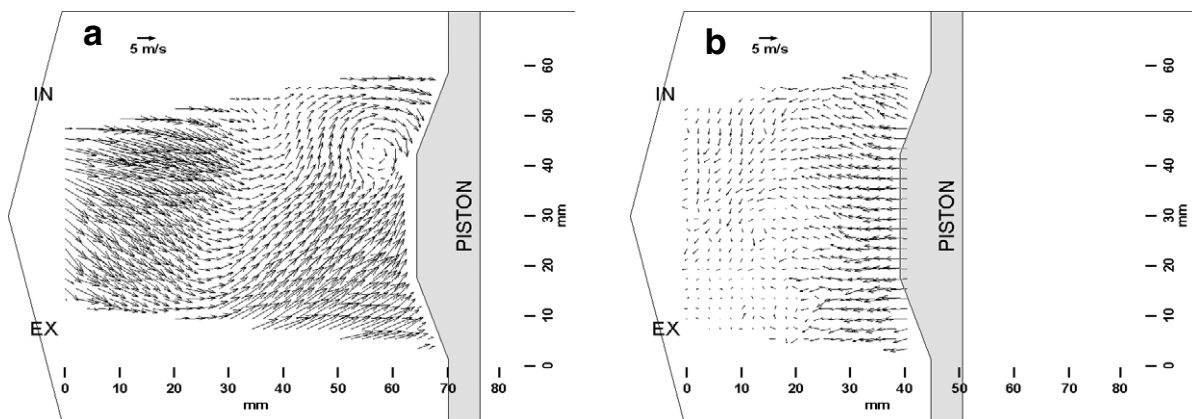

Figure 4. Case 1 (NVO, 150° duration, 1000 RPM). Vector fields captured at 135° (a) and 270° (b).
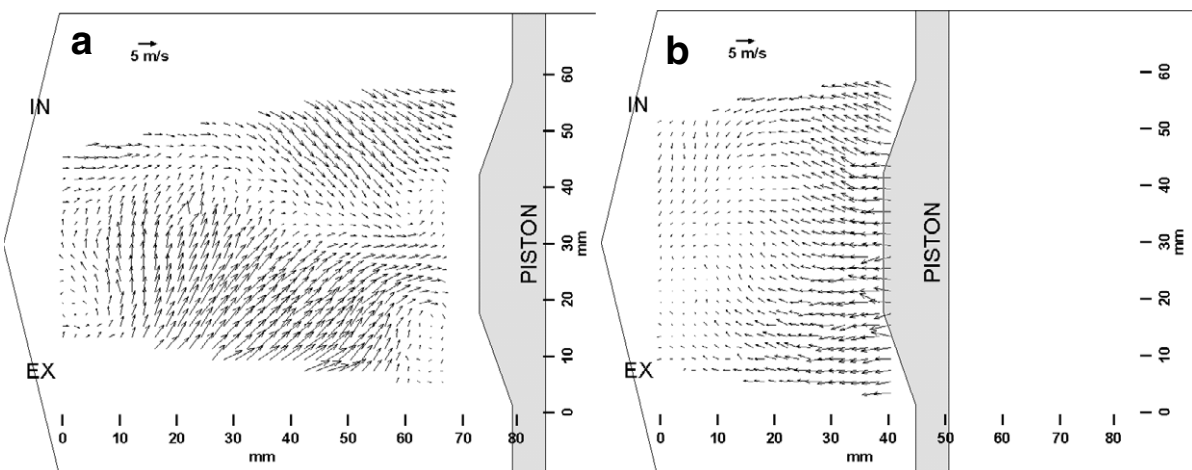

Figure 5. Case 2 (reduced negative valve overlap, 150° valve duration, 1000 RPM). Vector fields captured at 180° (a) and 270° (b).

Typically, significant variation was experienced on a cycle to cycle basis on the PIV testing, however, it is observed that the main characteristics of the flow are visible in the individual cycles, albeit not as clearly. Two differences were noted; first, although the bulk flow structures generally exist in the individual cycles, the velocities tend to vary significantly. Secondly, smaller flow structures (usually vortices) are observed in individual cycles, however since they are so short lived and unstable they do not appear in the mean flow field.

The large variations of the in-cylinder flow cycle to cycle also causes a large variation in the tumble ratio cycle to cycle. This is illustrated in **Figure 6**. The tumble ratio for the individual cycles varies from positive 0.6 to negative 0.6, a range of 1.2 ratios. There is minimal variation in tumble ratio whether calculated by taking the mean of the individual vector field tumble ratios, or if the tumble ratio is determined from the mean vector field. This finding is similar to that observed with typical SI valve events.
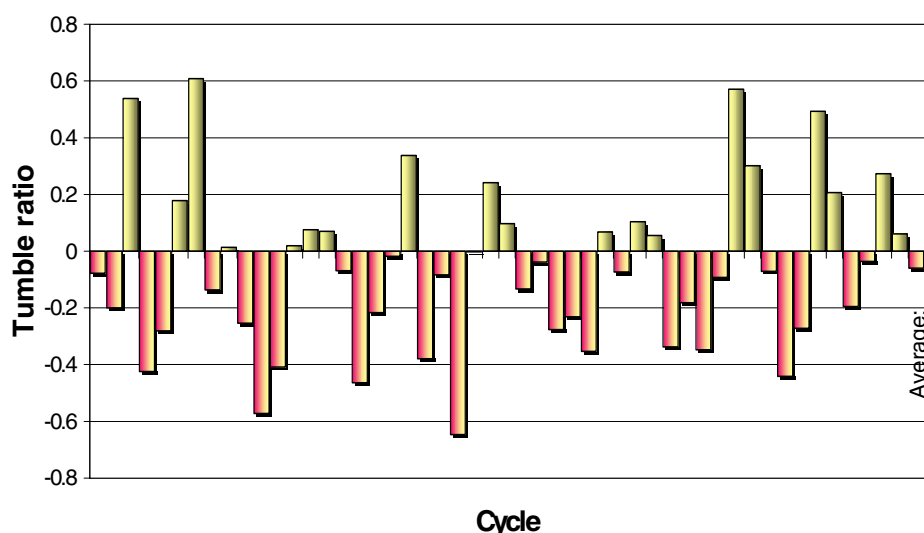

Figure 6. Cycle to cycle variation in tumble ratio at 180°, for case 1.

In general, it appears that when compared with previously investigated SI engine conditions, NVO condition generates an in-cylinder air motion that is less uniform and less stable.

3.2. Combustion Imaging

High-resolution combustion imaging was performed at 1° CA intervals starting before combustion initiation and finishing after complete visible chamber engulfment for various engine conditions.

3.2.1. Cycle to cycle variation

The high-resolution combustion imaging is particularly useful for yielding information on combustion area contours, combustion initiation centres and cycle-to-cycle variation in initial combustion development. Figure 7 provides a comparison of combustion areas where each image is captured at the same crank angle of 7° bTDC (but in different engine cycles) and integrated over a time period equivalent to one degree crank angle.

In this case the engine was operated at stoichiometric with natural gas as fuel. Intake temperature was held constant at 200°C and the in-cylinder pressure indicated load (IMEP) of 2.4 bar. Intensifier integration period was 167μs corresponding to 1°CA. Immediately obvious is the large variation in combustion contour shape between individual cycles.

Interestingly, for example the images labelled 4 and 5 in **Figure 7** show similar combustion area contour, however these are positioned differently in the chamber. Both frames have one large combusting zone and at least one smaller detached auto ignited combustion. It appears that in both frames these combusting zones are detached from the cylinder wall. Also noticeable is the large variation in pattern of the distribution of combustion areas between individual images. It can be a single relatively large burning area (as in frame 6), or several smaller areas (as in frame 3), while in each case the total combustion area is similar (9% ± 2.5%).
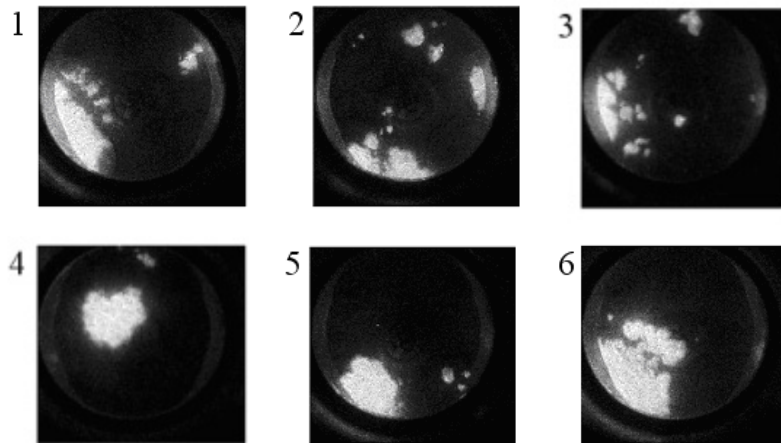
Figure 7. Combustion region structure and initiation imaged at 7°bTDC.

Finally, it is possible to compare the position in the chamber where the combustion initiation occurs. Investigation from a large number of cycles suggests that the dominant area of combustion initiation is the left hand side of the chamber (corresponding to the front of engine, between intake and exhaust valves). In general, however, combustion initiation with natural gas as a fuel appears random.

3.2.2. Combustion development
Imaging conducted at increasing crank angles, although from different cycles, permits a combustion development sequence to be built up. Such results are presented in **Figure 8**, where the engine was again operated at stoichiometric with natural gas as fuel. Intake temperature was held constant at 200°C and the in-cylinder pressure indicated load (IMEP) of 2.4 bar. Intensifier integration period was 167μs corresponding to 1°CA.
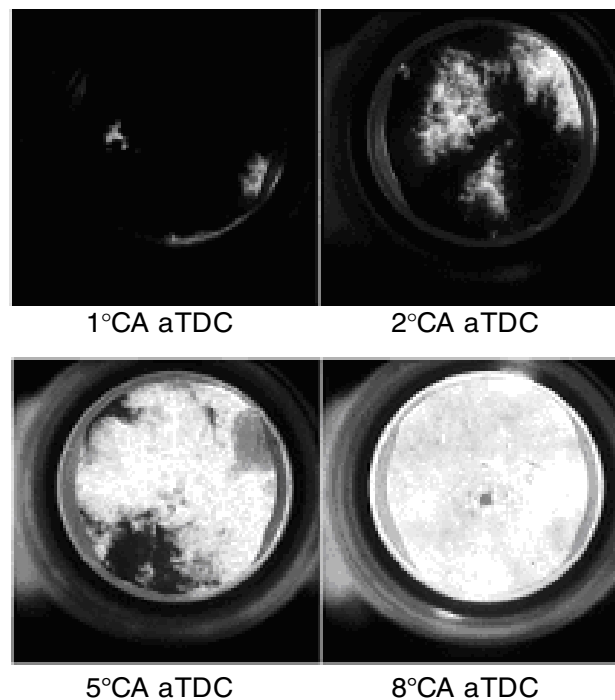

1°CA aTDC   2°CA aTDC

5°CA aTDC   8°CA aTDC

Figure 8. Combustion development.

A clear combustion development is obvious starting with multiple ignition sites and progressing to complete chamber engulfment. In this regard, various methods of image processing were performed; possibly the most informative were calculations of the area of the projected cylinder volume engulfed by combustion. This was performed by a simple threshold technique whereby pixel intensities above a threshold of 1.5% of the maximum grey level were assumed to be representing visible combustion, below that threshold they were not. Such results are presented in **Figure 9** (crosses) where they are compared to mass fraction burned (lines with no markers).

In this case the engine was operated at stoichiometric with natural gas or natural gas with hydrogen (H_2) addition (hydrogen replaced some of natural gas to maintain lambda=1 in volumetric ratio of 1:10) fuels as indicated (See [1,8] for purpose of H_2 addition). Intake temperature was held constant at 200°C and the in-cylinder pressure indicated load (IMEP) varied from 2.5 bar to 2.9 bar depending on combustion phasing. Intensifier integration period was 167μs corresponding to 1°CA.

Such an approach provides an opportunity to investigate how individual variables affect the combustion phasing and the rate of combustion development. In this context, **Figure 9** shows the effect of H_2 addition on combustion development. Comparing the crank timing corresponding to the 5% and 95% chamber area engulfed indicates that while the H_2 addition advances the early combustion development (5% area) by only 3°, it significantly accelerates the rate of combustion development as the 95% chamber engulfed can be seen to be approximately 8° advanced. This was not as evident in the fuel mass fraction burned plots where the H_2 addition advanced the timing of 5% mfb by 3° CA and the 95° burn by only 5° CA. Although it should be noted that the part of the combustion chamber near the cylinder wall is not visible due to the limitations of the window size, the uncertainty in estimating the total combustion area is not expected as significant as for spark-ignition engines because of the nature of the multi-point ignition of HCCI.
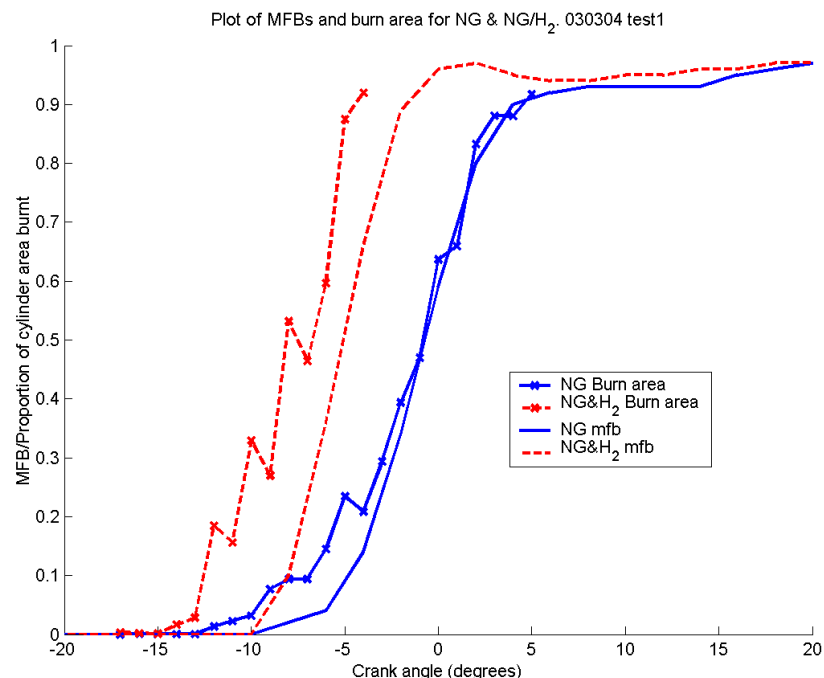

Figure 9. Comparison of burn area and MFB for NG HCCI, with and without H2 addition. (Combustion areas are average from 10 cycles, mfb average of 100 cycles)

4. Conclusions

An experimental investigation has been carried out in a specially designed optical engine operating in HCCI mode to study to the in-cylinder flow field and combustion development with negative valve overlap. The measurements using PIV and combustion imaging techniques have revealed the following:

- In contrast to the flow in SI engines with conventional positive valve overlapping, the negative valve overlap with reduced valve lift and duration generated intake flow velocities significantly higher than those found with typical positive overlapping valve strategies. For example at 1000RPM, the maximum magnitudes of the in-cylinder flow with NVO valve events were observed to be as high as around 20m/s (5 times mean piston speed) early in the intake stroke due to the reduced valve duration and lift. The flow velocity at the end of compression dropped to under 4 m/s (just under mean piston speed) during compression.
- Flow motion during intake was largely valve event and induction driven. During compression, the flow showed very little structure and was largely piston driven upward flow. Flow fluctuations were much stronger during the compression stroke, which are reflected by high cycle-by-cycle variations of tumble ratio.
- It was noted that with natural gas HCCI, multiple separate combustion sites were observed, with a slight tendency for initiations to occur towards one side of the chamber.
- It was shown that H_2 addition to natural gas advanced combustion initiation (timing of 5% area of chamber engulfed by combustion advanced by 3° CA), and the speed of combustion development also increased considerably (timing of 95% combustion area advanced by 8-9° CA). This was not as evident in the fuel mass fraction burned plots in which although the advance in 5% mfb timing due to H_2 addition is also approximately 3° CA, the 95% mfb advancement is only 5° CA. This indicates the effect of hydrogen as reaction promoter on both combustion initiation and burn rate.

5. Acknowledgments

6. References

[1]   Yap, D., Megaritis, A., Peucheret, S., Wyszynski, M. L., Xu, Hongming, (2004): "Effect of hydrogen addition on natural gas HCCI combustion", SAE Paper Number 2004-01-1972.

[2]   A. Hultqvist, M. Christensen, B. Johansson, M. Richter, J. Nygren, J. Hult and M. AldJn, (2002): "The HCCI Combustion Process in a Single Cycle – Speed Fuel Tracer LIF and Chemiluminescence Imaging", SAE Paper Number 2002-01-0424.

[3]   Wilson, T., Haste, M., Xu, H.M., Richardson, S., Yap, D., Megaritis, A., (2005): "In-cylinder Flow with Negative Valve Overlapping - Characterised by PIV Measurement, " SAE Paper Number 2005-01-2131.

[4]   P. Bryanston-Cross, M. Burnett, B. Timmerman, W. K. Lee & P. Dunkley (2000) "Intelligent diagnostic optics for flow visualization" Optics and Laser Technology, 32(7-8), pp. 641-654

[5]   E. L. Hines, D. D. Udrea, T. Wilson, P. Dunkley, M. Burnett & P. J. Bryanston-Cross (1999) "Application of fuzzy logic and neural networks to the automatic determination 2 and 3 dimensional PIV velocity distributions" SPIE 44th General Meeting, (Technical Conference 3783: Optical Diagnostics for Fluids/Heat/Combustion and Photomechanics for Solids)

[6]   M. Ronnback, W. X. Le & J. R. Linna (1991) "Study of Induction Tumble by Particle Tracking Velocimetry in a 4-Valve Engine". SAE paper 912376, Presented at SAE.

[7]   L. Koopmans, J. Wallesten, R. Ogink and I. Denbratt (2004): "Location of the First Auto-Ignition Sites for Two HCCI Systems in a Direct Injection Engine", SAE Paper Number 2004-01-0564.

[8]   Xu, H.M., Wilson, T.S., Richardson, S., Wyszynski, M.L., Megaritis, T., Yap, D., Golunski, S., James, D., (2004): "Extension of the boundary of HCCI Combustion using fuel reforming technology", SAE Paper Number 20045468.

[9]   A. Hultqvist, M. Christensen, B. Johansson, A. Franke, M. Richter and M. Aldén, (1999): "A Study of the Homogeneous Charge Compression Ignition Combustion Process by Chemiluminescence Imaging", SAE Paper Number 1999-01-3680.